

Site-Specific Backbone Dynamics from a Crystalline Protein by Solid-State NMR Spectroscopy

Nicolas Giraud,[†] Anja Böckmann,[‡] Anne Lesage,[†] François Penin,[‡] Martin Blackledge,[§] and Lyndon Emsley^{*†}

Laboratoire de Chimie, UMR 5182 CNRS/ENS, Laboratoire de Recherche Conventinné du CEA (no. 23V), Ecole Normale Supérieure de Lyon, 69364 Lyon, France, Institut de Biologie et de Chimie des Protéines, UMR 5086 CNRS/UCB, IFR 128 Biosciences Lyon-Gerland, 69367 Lyon, France, and Institut de Biologie Structurale Jean-Pierre Ebel CNRS/CEA/UJF, 38027 Grenoble, France

Received June 10, 2004; E-mail: Lyndon.Emsley@ens-lyon.fr

The determination of molecular dynamics in proteins is one of the key challenges in understanding their structure–function relationships. While great progress has been made in this field using solution-state NMR methods,¹ there are currently no experimental probes available that provide detailed information about local dynamics throughout solid proteins. In this context, nuclear spin relaxation times provide a direct and unambiguous measure of the presence of molecular dynamics in solids, which cannot be confused with static structural disorder. The link between nuclear relaxation times in solids and motion has been established for decades,^{2,3} and several deuterium NMR line shape and relaxation^{4–6} studies have been performed on solid proteins in the past. Cole and Torchia⁷ have also measured nitrogen-15 relaxation times. In these studies, however, it was not possible to obtain widespread multiple site-specific information, nor was it possible to obtain information about the variation of mobility from one part of the molecule to another. This internal information is crucial to most modern models of protein interactions and function.

The introduction of microcrystalline protein samples,^{8–12} as well as substantial improvements in the sensitivity and resolution of multidimensional solid-state NMR experiments, has led to very rapid recent progress being made in this field, resulting in the first complete assignments of proteins in the solid state^{9,10} and the first three-dimensional structure.¹³ This progress provides high-resolution, high-sensitivity spectra and opens up the perspective of measuring site-specific relaxation times as probes of local dynamics.

Here we present measurements of nitrogen-15 nuclear longitudinal relaxation rates (R_1) in a microcrystalline sample of the protein Crh⁹ and provide a qualitative description of the site-specific backbone dynamics in the solid state.

Figure 1a shows the pulse sequence used to measure site-specific nitrogen-15 R_1 's, observed in a 2D ^{15}N – ^{13}C correlation spectrum (the pulse sequence and phase cycle are available on our web site¹⁴ or upon request). The sequence is based on a double cross-polarization technique using adiabatic passage through the Hartman–Hahn condition (APHH)¹⁵ for the step from ^{15}N to ^{13}C to ensure maximum transfer efficiency. After cross-polarization from protons to nitrogen, a 90° pulse rotates the magnetization to the z -axis where it undergoes spin–lattice relaxation during the variable delay τ . After a second 90° pulse, the ^{15}N chemical shift is recorded during t_1 . The magnetization is then transferred from ^{15}N to ^{13}C , and the ^{13}C free induction decay is acquired in t_2 . Cosine modulated (CM) heteronuclear decoupling was used in both dimensions.^{16–18}

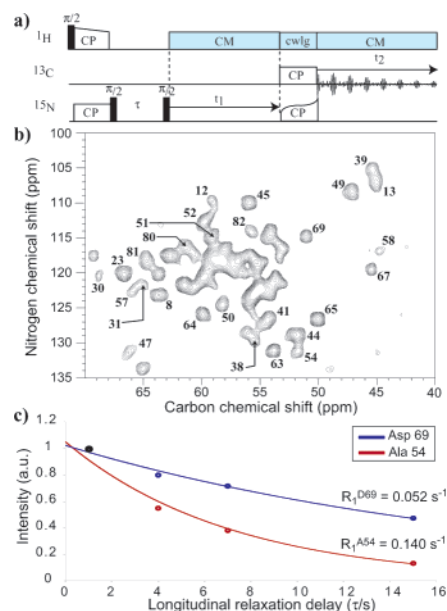


Figure 1. (a) Pulse sequence used to record the nitrogen-15–carbon-13 correlation spectra, resulting in spectra of type shown in (b) for Crh. The ^{15}N – ^{13}C CP step was performed using a linear ramp (100 to 70% of rf field strength) on the ^{15}N channel, with a 2.3-ms CP period and an rf field strength of 45 kHz for ^{15}N . The 7-ms ^{15}N – ^{13}C cross-polarization step used an adiabatic amplitude modulated tangential ramp on the nitrogen channel with rf field strengths of about 50 and 40 kHz for ^{13}C and ^{15}N . The rf field strengths for the 90° pulses were 80 kHz for ^{15}N and 50 kHz for ^{13}C . The proton decoupling field was set to 80 kHz for CM and cwlg.^{16–18} Quadrature detection was obtained with TPPI. Each of the 220 increments in t_1 were acquired with 96 scans and a 3-s recycle delay between scans, with maximum acquisition times of 12.2 ms in t_1 and 15 ms in t_2 . Data were processed using zero-filling up to 1024 points in t_1 , and 2048 points in t_2 , a square cosine filter and automatic baseline correction in both dimensions. The $\tau = 1 \text{ s}$ spectrum was recorded in 24 h using about 8 mg of protein. In (c) we show two of the resulting decay curves measured using four values of the relaxation delay τ and which have been renormalized so that the first points ($\tau = 1 \text{ s}$) are of equal intensity.

The resulting heteronuclear correlation spectrum provides both N–CO and N–CA correlations.

Experiments were carried out on a Bruker Avance 500 MHz spectrometer using a 4-mm triple-tuned CPMAS probe, at a spinning speed of 10 kHz, on a microcrystalline, uniformly labeled [^{15}N , ^{13}C] sample of the protein Crh in its domain swapped dimeric form ($2 \times 10.4 \text{ kDa}$).^{9,19,20} The sample preparation has been described in detail elsewhere.⁹ The probe temperature was set to -6°C , which corresponds to an effective sample temperature about $+7.5^\circ\text{C}$, the difference being principally due to heating from friction during sample spinning. A series of 4 spectra, with τ delays

[†] Laboratoire de Chimie, UMR 5182 CNRS/ENS, Laboratoire de Recherche Conventinné du CEA (no. 23V), Ecole Normale Supérieure de Lyon.

[‡] Institut de Biologie et de Chimie des Protéines, UMR 5086 CNRS/UCB.

[§] Institut de Biologie Structurale Jean-Pierre Ebel CNRS/CEA/UJF.

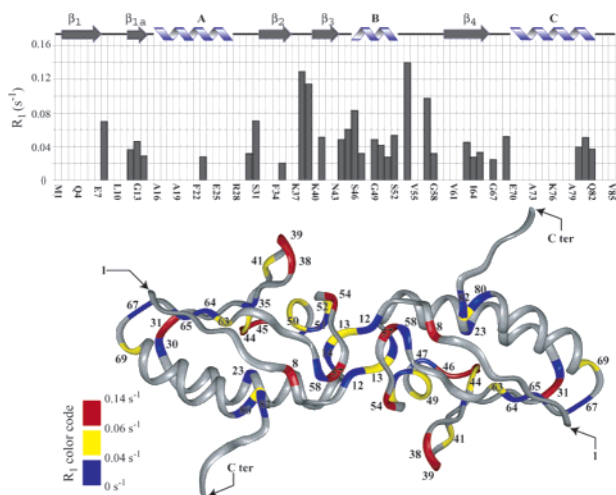


Figure 2. Bar graph of measured R_1 vs residue number obtained from experiments using the sequence of Figure 1, as well as a representation of the secondary structure. Numerical values of R_1 are given in a table in the Supporting information. The X-ray crystal structure of the protein²⁰ is shown color coded according to the value of R_1 as shown in the legend.

of, respectively, 1, 15, 7, and 4 s were recorded. The 1-s spectrum was re-recorded between each of the other spectra to provide an internal reference for the possibility of slight changes in cross-polarization efficiency from one experiment to another. R_1 data were obtained from peak intensities. (See Supporting Information for further details.)

Figure 1b shows a typical 2D spectrum ($\tau = 1$ s) for Crh. The cross-polarization times were optimized for maximum transfers from each nitrogen to only its neighboring carbons (C_α and C'). From these spectra, we could obtain unambiguous relaxation data from 30 resolved ^{15}N – ^{13}C cross-peaks (assignment shown on spectrum).

Figure 1c shows typical decay curves measured for Ala 54 and Asp 69. The quality of curve fits allows a clear distinction between different values of R_1 observed over a range between 0.15 s^{-1} and about 0.02 s^{-1} (corresponding to relaxation times $T_1 = 1/R_1$ of between 6 and 50 s) with an accuracy estimated at about $\pm 0.005\text{ s}^{-1}$ (except Leu 35 and Ser 46 whose uncertainty is about 0.01 s^{-1} , because of the low signal-to-noise ratio of the corresponding peaks).

Figure 2 shows the R_1 values measured for Crh. First, we remark that there is a substantial variation in relaxation rates from one residue to another. This clearly indicates that there are variations in mobility along the backbone in the solid state.

Even if a quantitative analysis cannot yet be carried out, some tendencies can be noted. Lowest R_1 values correspond mainly to residues located in regular secondary structures: Val 23, Ile 47, Met 51, Tyr 80, Val 81, and Gln 82 are in α -helices, and Leu 14, 35, 63, Ile 64, and Ala 65 are in β -strands. Conversely, loop residues that are expected to be more mobile show, in general, higher R_1 values. Residues Glu 38 and Gly 39 in a protruding loop show particularly fast R_1 , indicating higher flexibility as was previously observed in solution for the monomeric form.²¹ Interestingly, we know that these residues also have high B factors from the X-ray study.²⁰ These variations in R_1 are coherent with expected fluctuations of internal mobility.

The fast R_1 for Ala 54 is particularly notable. This residue undergoes a major dislocation on domain swapping,²⁰ and here appears to remain mobile in the dimer. Finally, we note that the active site residue Ser 46, which is phosphorylated by HprK/P, seems to belong to the more mobile residues.

We have also measured longitudinal relaxation rates for (unassigned) Gln N ϵ 2 and Asn N δ 2 side-chain nitrogens that are in the range between 0.25 and 0.12 s^{-1} .

In conclusion, we observe substantial differences (up to a factor 7) in R_1 along the backbone. It is apparent that there is a strong correlation between measured relaxation rates and a simple but coherent preliminary picture of internal mobility, with increased mobility providing faster R_1 . In particular, we find increased mobility for residues that are not in regular secondary structures, whereas the rates measured for residues in α -helices or β -sheets show less mobility. Since the data were measured at one field, we cannot identify the nature of the differential dynamics occurring here, or distinguish between time scale and motional amplitude effects. Nor can we determine any perturbations that could arise from variations in parameters such as local proton density or due to nearby methyl groups, for example. A more detailed quantitative treatment is perfectly possible³ but requires more data to provide constraints on the particular motional model and spectral density function.²

It is worth noting that the solid state provides an extremely direct route to internal mobility, since the overall tumbling of the molecule, which complicates solution state modeling, is absent.

Acknowledgment. We are grateful to Sabine Hediger for stimulating discussions. This work was supported in part by the French Research Ministry ACI 032570.

Supporting Information Available: Table of measured values obtained for R_1 and details of the processing procedure. This material is available free of charge via the Internet at <http://pubs.acs.org>.

References

- Brüschweiler, R. *Curr. Opin. Struct. Biol.* **2003**, *13*, 175–183.
- Spiess, H. W. In *NMR Basic Principles and Progress*; Springer-Verlag: Berlin Heidelberg, New York, 1978; Vol. 15.
- Torchia, D.; Szabo, A. *J. Magn. Reson.* **1982**, *49*, 107–121.
- Rozovsky, S.; McDermott, A. E. *J. Mol. Biol.* **2001**, *310*, 259–270.
- Palmer, A. G.; Williams, J.; McDermott, A. *J. Phys. Chem.* **1996**, *100*, 13293–13310.
- Mack, J. W.; Usha, M. G.; Long, J.; Griffin, R. G.; Wittebort, R. *J. Biopolymers* **2000**, *53*, 9–18.
- Cole, H. B. R.; Torchia, D. *Chem. Phys.* **1991**, *158*, 271–281.
- Martin, R. W.; Zilm, K. W. *J. Magn. Reson.* **2003**, *165*, 162–174.
- Böckmann, A.; Lange, A.; Galinier, A.; Luca, S.; Giraud, N.; Juy, M.; Heise, H.; Montserret, R.; Penin, F.; Baldus, M. *J. Biomol. NMR* **2003**, *27*, 323–339.
- Pauli, J.; Baldus, M.; van Rossum, B.-J.; De Groot, H.; Oschkinat, H. *ChemBioChem* **2001**, *2*, 272–281.
- McDermott, A.; Polenova, T.; Böckmann, A.; Zilm, K. W.; Paulson, E. K.; Martin, R. W.; Montelione, G. T.; Paulsen, E. K. *J. Biomol. NMR* **2000**, *16*, 209–219.
- Igumenova, T. I.; Wand, A. J.; McDermott, A. E. *J. Am. Chem. Soc.* **2004**, *126*, 5323–5331.
- Castellani, F.; van Rossum, B.; Diehl, A.; Schubert, M.; Rehbein, K.; Oschkinat, H. *Nature* **2002**, *420*, 98–102.
- Emsley, L. Nuclear Magnetic Resonance. <http://www.ens-lyon.fr/STIM/NMR>.
- Baldus, M.; Geurts, D. G.; Hediger, S.; Meier, B. H. *J. Magn. Reson., Ser. A* **1996**, *118*, 140–144.
- De Paepe, G.; Giraud, N.; Lesage, A.; Hodgkinson, P.; Bockmann, A.; Emsley, L. *J. Am. Chem. Soc.* **2003**, *125*, 13938–13939.
- De Paepe, G.; Hodgkinson, P.; Emsley, L. *Chem. Phys. Lett.* **2003**, *376*, 259–267.
- De Paepe, G.; Elena, B.; Emsley, L. *J. Chem. Phys.* **2004**, *121*, 3165.
- Galinier, A.; Haiech, J.; Kilhoffer, M. C.; Jaquinod, M.; Stulke, J.; Deutscher, J.; Martin-Verstraete, I. *Proc. Natl. Acad. Sci. U.S.A.* **1997**, *94*, 8439–8444.
- Juy, M.; Penin, F.; Favier, A.; Galinier, A.; Montserret, R.; Haser, R.; Deutscher, J.; Böckmann, A. *J. Mol. Biol.* **2003**, *332*, 767–776.
- Favier, A.; Brutscher, B.; Blackledge, M.; Galinier, A.; Deutscher, J.; Penin, F.; Marion, D. *J. Mol. Biol.* **2002**, *317*, 131–144.

JA046578G